Ion-Image State as an Intermediate in the Surface Generation of Photocurrent in Solution

Alfred Prock,*[1] Robert Zahradnik, and Sara Grassino

Contribution from the Chemistry Department, Boston University, Boston, Massachusetts 02215. *Received March 6, 1972*

Abstract: The surface-generated photoconduction of rubrene in benzene solution under visible radiation is interpreted in terms of an ion-image state as an intermediate species. Electrostatic interaction of these transient species creates a barrier to charge transfer at the surface and produces a saturation of photocurrent with light intensity. The existence of the ion-image state is employed to explain the field and intensity dependence of the photocurrent saturation.

Photoconduction by solutions of rubrene (5,6,11,12-tetraphenyltetracene) in benzene has been studied under low-energy, visible excitation with the aim of observing and characterizing the intermediate states in charge generation that occur at the electrode. This system is particularly useful in this respect since there is both high efficiency of charge transfer to the electrode and negligible interference from the triplet state of rubrene. In benzene, rubrene has a quantum efficiency of nearly unity,[2] with a radiative lifetime of 16.4 nsec,[3] and the triplet state can be prepared in significant concentration by an energy transfer process[4] and not by intersystem crossing.

This paper reports on observations including charge generation in steady state and after a pulse of light, which indicate the presence of an intermediate state at the positive transparent electrode. Charge injection after a pulse was noted earlier[5] in a study of space charge modified currents in the same system. In the present paper the quantitative measurements of "lifetime" of the state and its field strength dependence are made. The existence of this state is used to explain by means of a kinetic analysis the low field-strength saturation of photocurrent with light intensity and the dependence of saturation on applied field strength. It is also used to explain the 1.5 power of field-strength dependence of photocurrent in the region of linear-intensity dependence. The saturation is consistent with a model where the dipole fields of the transient adsorbed ion-image pairs, which surround a given excited rubrene molecule at the electrode plane, produce an electrostatic barrier at the molecule which hinders charge transfer to the electrode.

Experimental Section

The apparatus and setup for steady-state and pulse measurements is similar to one described earlier.[6] A 450-W xenon lamp is the source for steady-state and chopped-light experiments, and for the present pulse measurements a Strobe Flash (General Radio 1539-A) was used. This produces a maximum energy of about 0.4 J with a half-rise time of less than 1 μsec. In addition because of the repetitive flash the same signal-averaging capabilities of the system could be used for pulse as well as chopped-light measurements. Schott interference filters were used to isolate the visible bands at 436, 497, 546, 606, 666, and 740 nm, along with 1 cm of saturated $NaNO_2$ and a circulating water filter as described.

Rubrene was obtained from Aldrich and was of highly variable quality. Temperature gradient vacuum sublimation and thin layer chromatography revealed significant amounts of impurities in their later batches. Sufficient initial purification was achieved by slow crystallization in a distillation apparatus where the benzene solvent was replaced by 2-propanol. This was repeated as necessary and followed by extensive chromatography on silica–alumina using pentane as solvent by the method of Sangster and Irvine.[7] All operations were done in the dark to prevent formation of the photooxide. The best indication of purity turned out to be the level of photoconduction under fixed conditions. Extensive purification was required to achieve a reasonably reproducible and high level of response. The product consisted of small crystals, deep red in color.

The photoconductivity cell was similar to that previously described, except that it was all Pyrex with fixed electrode spacing. Individual cell spacing varied from 0.10 to 0.40 mm, and was vacuum tight and bakeable. Electrode material was evaporated stannic oxide. Electrode capacitance and dissipation factor were measured when the cell was filled with solution, using a General Radio 1608A bridge. The dissipation factor was interpreted as a measure of the effective series resistance of all internal electrode connections plus stannic oxide films, and was acceptable when it corresponded to a cell time constant of less than 0.5 μsec.

Benzene was prepared by careful distillation in a nitrogen atmosphere over $LiAlH_4$. This was followed by two bulb-to-bulb sublimations on a high vacuum line before entry into the cell which contained rubrene sealed into a side arm. The filled cell was drawn from the line in the usual manner.

Results

Rubrene in benzene solution shows visible absorption peaks at 464 nm ($4.2 \times 10^3\ M^{-1}\ cm^{-1}$), 494 nm ($8.0 \times 10^3\ M^{-1}\ cm^{-1}$), and 528 nm ($8.5 \times 10^3\ M^{-1}\ cm^{-1}$). Its solubility in excess of $3 \times 10^{-2}\ M$ at room temperature is enough so that the penetration depth of 546-nm light is 0.004 cm. Under these conditions simple reversal of electrode polarity in the sandwich type cell is sufficient to show that only the anode region is involved in photoionization. For example, in a typical case the photocurrent is reduced two orders of magnitude if light is incident on the negative electrode. The high intensity of light provided by interference filters is required for solution work in contrast to crystal measurements because of the relatively small ratio of diffusion length of a singlet exciton to absorption depth of light, typically around 10^{-4}. This is the fraction of excited singlets which can interact with the

(1) Author to whom correspondence should be addressed at the Department of Chemistry, Boston University, Boston, Mass. 02215.
(2) E. J. Bowen and A. H. Williams, *Trans. Faraday Soc.*, **35**, 44 (1939); see also "Photophysics of Aromatic Molecules," J. B. Birks, Wiley, New York, N. Y., 1970.
(3) S. J. Strickler and R. A. Berg, *J. Chem. Phys.*, **37**, 814 (1962).
(4) A. Yildiz, P. T. Kissinger, and C. N. Reilley, *ibid.*, **49**, 1403 (1968).
(5) R. G. Romanets, A. Prock, and R. Zahradnik, *ibid.*, **53**, 4093 (1970).
(6) A. Prock and R. Zahradnik, *ibid.*, **49**, 3204 (1968).
(7) R. C. Sangster and J. W. Irvine, Jr., *ibid.*, **24**, 670 (1956).

Table I

kV_{app}	0.50	0.77	1.01	1.33	1.56	1.82	2.03	2.37	2.62
$t_{1/2}$, μsec (error ±5 μsec)	59	47	48	42	43	38	37	29	24

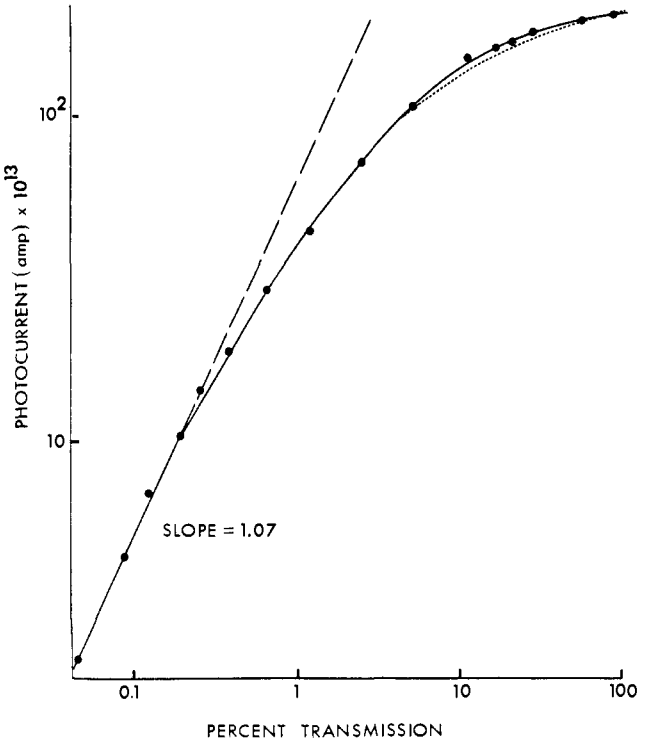

Figure 1. Solid line: steady-state photocurrent *vs.* light intensity (497 nm) for rubrene (1.1×10^{-2} *M*) in benzene. Electrode spacing is 0.021 cm, applied voltage is 112 V, light flux at 100% transmission is 10^{15} photons sec^{-1} cm^{-2}. Dotted line: theoretical curve, eq 7, see text.

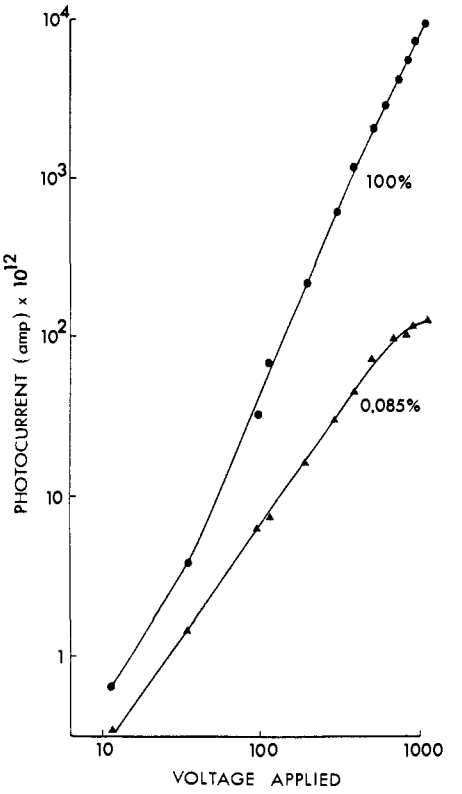

Figure 2. Steady-state photocurrent *vs.* applied voltage for rubrene (3.3×10^{-2} *M*) in benzene. Wavelength is 546 nm, electrode spacing is 0.021 cm, and 100% transmission corresponds to 6×10^{15} photons sec^{-1} cm^{-2}.

anode.[8,9] The six wavelength bands which we have used are sufficient to reveal that the photoconduction spectrum essentially follows the absorption spectrum with a tail which at 666 nm is down two orders of magnitude. Stability and reproducibility of measurements for a given solution were excellent. The same cell could be used for extensive measurements, both steady state and pulse, over periods of months with no apparent change.

Figure 1 (solid line) is a plot of steady-state photocurrent *vs.* light intensity for 497-nm light for a solution of rubrene of 1.1×10^{-2} *M* concentration. Balzer neutral density filters were used, and light intensity is plotted as per cent transmission with 100% corresponding to 10^{15} photons sec^{-1} cm^{-2}. Applied potential was 112 V across an electrode spacing of 0.021 cm. The initial slope is 1.07, which indicates essentially linear intensity dependence at the low range of intensity. A very strong apparent "saturation" of photocurrent is seen at high light intensity.

Chopped light experiments similar to one described earlier[5] were done. For a solution of 3.3×10^{-2} *M* and 497-nm light, the log–log plot of initial rise rate *vs.* light intensity yields a slope of 1.03. This is taken to indicate a single photon charge generation step.

Figure 2 demonstrates the dependence on applied voltage of the steady-state photocurrent saturation. It is a log–log plot of photocurrent *vs.* applied voltage at two widely different intensities, 100 and 0.085% of full intensity. The rubrene solution was 3.3×10^{-2} *M*, wavelength 546 nm, intensity 6×10^{13} photons sec^{-1} cm^{-2}, and electrode spacing 0.021 cm. The divergence between the curves is apparent at increasing voltage. At 1000 V the curves are separated by two orders of magnitude and light intensity still differs by three orders of magnitude. The divergence indicates a straightening out with higher applied voltage of curves similar to Figure 1. Note that Figure 2 shows greater saturation at higher concentration and higher light intensity.

Table I lists the results of pulse measurements with the General Radio Strobe Flash on a concentrated solution of rubrene in a cell with spacing 0.04 cm. The half-rise time of photocurrent, $t_{1/2}$, has been corrected in a simple way by subtracting out all the instrumental half-rise times. Flash and cell rise times were mentioned before and account for 1.5 μsec. The largest time was associated with the RC time constant of the preamplifier and was measured directly with the aid of a square-wave generator. For example, with a 0.47 Megohm input resistance across the Keithley Model 103 amplifier the half-rise time as measured on the X–Y recorder at the output was 13.5 μsec. The decrease in

(8) B. J. Mulder, *Philips Res. Rep., Suppl.*, 4 (1968).
(9) H. Killesreiter and H. Baessler, *Chem. Phys. Lett.*, **11**, 411 (1971).

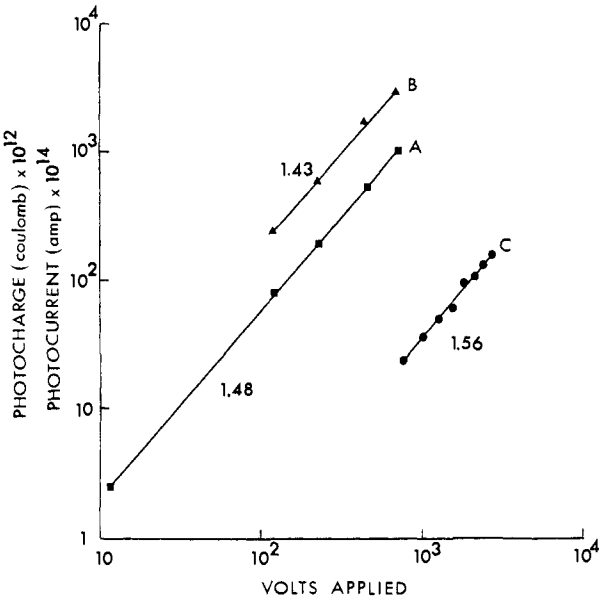

Figure 3. Rubrene solution (3×10^{-2} *M*) in benzene (A). Steady-state photocurrent *vs.* applied voltage at low light intensity. Wavelength is 606 nm, electrode spacing is 0.020 cm. (B) Similar to graph A, but wavelength is 666 nm. (C) Photocharge *vs.* applied voltage in a flash experiment using white light. Electrode spacing is 0.04 cm. The slope for each curve is indicated on the figure.

half-rise time with increasing applied potential is apparent. The results were not significantly dependent on incident wavelength and were therefore taken with white light in order to produce sufficient signal to noise ratio.

The results of steady-state measurements are not shown but behave differently with respect to their time dependence. Currents do not reach steady state until time periods from a minute to several minutes for both rise and decay. Further, for the same solution under test in both steady state and chopped light, where the only change is presence or absence of a chopper, the steady-state currents are an order of magnitude larger. This indicates a rise which is very slow in comparison to the time scale (milliseconds) of the chopped-light experiments where an apparent steady state is reached for both the light and dark conditions. Although our results indicate that this is associated with formation of the intermediate state, the time dependence of the pulsed-light experiments has been stressed here. This was done because the increase in photocurrent in the latter case continues for a time which is long compared with flash duration, but short compared with dielectric relaxation in the liquid (which is at least several seconds), and therefore clearly must come from an intermediate species.

Figure 3 shows additional data to determine voltage dependence of photoresponse in regions far removed from saturation; *i.e.*, where photocurrent is linear in light intensity. Figures 3a and 3b are for steady-state photocurrent, and Figure 3c is for pulsed measurements. Solutions were 3×10^{-2} *M*. Figure 3a is for 606-nm light of 5.2% full intensity and electrode spacing of 0.020 cm. The slope of the log–log plot, 1.48, is the experimentally determined exponent for the voltage dependence of photocurrent. Figure 3b is similar with wavelength of 666 nm, 100% full intensity. The slope of the log–log plot is 1.43. Figure 3c is a log–log plot of integrated charge, *Q*, which flows in a pulsed light experiment as a function of applied voltage. White light was used, and electrode spacing was 0.04 cm. The areas under photocurrent *vs.* time curves were obtained from the X–Y recorder plots of the signal averaging system. The slope of this plot is 1.56.

Discussion

The photoconduction of benzene solutions of rubrene appears to involve an intermediate species which is capable of injecting charge into the solution for times that are long compared with the lifetime of singlet rubrene in solution. The low rate of intersystem crossing to the triplet state and the lack of quenching by oxygen rules out triplet-state involvement. The most likely species is the one which results when the singlet exciton transfers its charge to the electrode. The positive ion and its image charge, *i.e.*, an adsorbed ion pair, is expected to be more stable than an ion pair in solution because of the extra stability gained by the electron within the energy states of the electrode. The fate of the charge pair logically appears to be either recombination or dissociation into separated charge. The data presented in Table I for flash excitation are consistent with a model of a field-assisted dissociation of the adsorbed ion pair, and show a decrease in half-rise time of a factor greater than 2 over the range of applied voltage from 0.50 to 2.62 kV. It is important to note that the half-rise time does not occur because of diffusion of rubrene triplets to the anode from the region of the absorption depth of the solution. This cause of delayed charge production has been described for the solid state[10] and can be important even if intersystem crossing is fractionally small as long as the extinction depth of the light is large compared with the diffusion length of the triplet. That is, the relative availability of triplets to singlets in producing photocurrent is the ratio of the products of concentration of the species times its diffusion length, and the latter number is proportional to the square root of the species lifetime. This could be significant for rubrene where the extinction depth is at least 0.004 cm. However, the lack of oxygen quenching, and the existence of the voltage dependence of half-rise time eliminates triplet diffusion as the mechanism of delayed charge production.

The existence of the intermediate adsorbed ion pair can be used to explain in a very reasonable way the strong saturation of photocurrent with increasing light intensity as shown by Figure 1, and the decrease of saturation with increasing applied voltage, Figure 2. It is impossible to explain the saturation on the basis of quenching in the bulk of solution or on the basis of energy transfer to the electrode surface. In the latter case, although the lifetime of the excited state is lowered relative to its value in the bulk,[11] it is independent of light intensity, and one is not able to account for decreased yield as seen in the figures. Bulk quenching is ruled out simply because such a small slope at high intensity is unaccountable without involving cooperation between many molecules. For example, a dominating bimolecular quenching process would produce a slope of 0.50, and a slope of 0.33 would require a trimolecular

(10) H. Killesreiter and R. Braun, *Phys. Status Solidi B*, **48**, 201 (1971).
(11) H. Kallmann, G. Vaubel, and H. Baessler, *ibid.*, **44**, 813 (1971).

process, etc. Singlet–singlet quenching is ruled out on the basis that the large absorption depth produces a singlet concentration of the order of 10^{-10} M. Combination of this concentration with a bimolecular rate constant even as high as 10^{10} M^{-1} sec^{-1} leads to an effective lifetime of 1 sec, which is far longer than the singlet lifetime.

On the other hand the existence of adsorbed ion pairs produces at any given ion pair a potential barrier from the dipole fields of the others which hinders its dissociation into free charges. The calculations given below start with a distribution of adsorbed ion pairs on a plane. The ion pairs are treated as point dipoles whose configuration is taken to be essentially that of a two dimensional lattice. A calculation presented in the Appendix justifies this assumption. The back field from the lattice must be overcome when the ion pair forms by electron transfer and it is incorporated into a Boltzmann exponential term in the photocurrent expression. It turns out that this term leads to a saturation in the photocurrent very similar to that observed experimentally.

The kinetic scheme consists of only three equations. The first is the singlet generation step where all bimolecular quenching terms are omitted, and all real and effective unimolecular terms are described by a single lifetime, τ. The second describes the buildup of adsorbed positive ions at the electrode plane by charge transfer from rubrene excited singlets which move to the electrode across the diffusion length of about 50 Å in the liquid. Recombination destroys some ion pairs, and free ions are produced by field-assisted dissociation of a fraction of the adsorbed ion pairs. The last equation describes the field assisted dissociation. The equations are

$$\frac{\partial[\mathrm{R}^*]}{\partial t} = \epsilon C I_0 e^{-\epsilon C x} - \frac{[\mathrm{R}^*]}{\tau} + D\frac{\partial^2[\mathrm{R}^*]}{\partial x^2} \qquad (1)$$

$$\frac{\partial[\mathrm{R_w}^+]}{\partial t} = Dk_2\frac{\partial[\mathrm{R}^*]}{\partial x}\bigg|_{x=0} - k_3[\mathrm{R_w}^+] - \frac{\partial[\mathrm{R}^+]}{\partial t}\bigg|_{x=0} \qquad (2)$$

$$\frac{\partial[\mathrm{R}^+]}{\partial t}\bigg|_{x=0} = k_4(V)\cdot[\mathrm{R_w}^+] \qquad (3)$$

where R*, $\mathrm{R_w}^+$, and R^+ refer to excited rubrene singlets, adsorbed cations, and free rubrene cations, respectively; D is the diffusion coefficient for R*, and the wall is located at $x = 0$. The constant $k_4(V)$ is the field-dependent dissociation rate constant; ϵ is the molar absorption coefficient, C is rubrene concentration, and I_0 is initial light intensity.

With the model of complete quenching of excited rubrene singlets at the wall, then under steady-state illumination the solution of eq 1 is

$$[\mathrm{R}^*] = \frac{\epsilon C\tau I_0}{1 - (\epsilon C\sqrt{D\tau})^2}(e^{-\epsilon C x} - e^{-x/\sqrt{D\tau}}) \qquad (4)$$

and the flux of singlets to the wall in steady state is

$$+D\frac{\partial[\mathrm{R}^*]}{\partial x}\bigg|_{x=0} = I_0\frac{\sqrt{D\tau}}{\frac{1}{\epsilon C} + \sqrt{D\tau}} \approx \epsilon C\sqrt{D\tau}I_0 \qquad (5)$$

in agreement with ref 8. The last approximation follows because the extinction depth of light, $(\epsilon C)^{-1}$, is much greater than the diffusion length of the singlet exciton ($\sqrt{D\tau}$). These distances are of the order 4×10^{-3} and 10^{-6} cm, respectively.

The constant k_2 includes the effect on the adsorbed ion plus image charge, or dipole, of the surrounding dipoles. This effect is in the direction to create a potential barrier towards electron transfer from excited rubrene to the electrode. The corresponding factor takes the form $\exp[-(1/kT)/\Sigma_i m^2/l_i^3]$, where m is the dipole moment of the charge pair, and l_i is the separation distance between pairs. A similar factor must be included for the effect of the applied field. This is in a direction to lower the potential barrier for electron transfer. For small applied voltage this effect is normally expected to be small because of the very small ratio of barrier thickness to electrode separation distance. This is, the change in barrier height would be this ratio multiplied by applied voltage, under the assumption of a geometric field. With 100 V applied and a barrier thickness of the order of Ångströms, and electrode spacing of 10^{-2} cm, the change in barrier potential would only be tenths of a millivolt. However, it is to be expected that although the field is essentially its geometric value in the bulk, it will be larger than this value at the electrode surface. This is an effect of the finite thickness of the electrical double layer in such highly resistive media, and the dependence of this thickness on applied field. An estimate of this effect has been made which shows that significant reduction of double-layer thickness occurs for voltages of the order of hundreds of volts.[12] Therefore, significant reduction of the potential barrier height for electron transfer can occur in this region of applied voltage. We will indicate this lowering of the barrier by $f(V)$, and specify only that it is vanishingly small at small applied voltage and becomes appreciable at higher applied voltage. At very high voltages the concentration of adsorbed dipoles is negligible because of the high rate of photocurrent production and the barrier height is essentially zero. Then $f(V)$ makes no contribution to further lowering of the barrier. Therefore, the factor, $\exp[f(V)/kT]$ is to be included in k_2 and will be appreciably greater than unity only for the middle range of applied voltage.

To evaluate the summation in the exponential, a lattice model is employed where the number of effective nearest neighbors is 7 (see Appendix), and the average separation distance is $[\mathrm{R_w}^+]^{-1/2}$. Then

$$k_2 = k_2' \exp\left\{-\frac{7m^2}{kT}[\mathrm{R_w}^+]^{3/2} + \frac{f(V)}{kT}\right\} \qquad (6)$$

A steady-state solution can be obtained by combining eq 2 and 3 and setting the left side of eq 2 equal to zero to express the constancy of adsorbed ion-pair concentration. The result valid for dc measurements is

$$[\mathrm{R_w}^+] = \frac{k_2'}{k_3 + k_4(V)} I_0\epsilon C\sqrt{D\tau}\exp\left\{-\frac{7m^2}{kT}[\mathrm{R_w}^+]^{3/2} + \frac{f(V)}{kT}\right\} \qquad (7)$$

For the stationary case photocurrent, I_{ph}, is $\mathrm{d}[\mathrm{R}^+]/\mathrm{d}t$. This can be related to the adsorbed ion-image concentration, $[\mathrm{R_w}^+]$, by eq 3. The rate constant, $k_4(V)$, is field dependent and is written to include the 1.5 power of

(12) A. Prock and W. A. LaVallee, *J. Phys. Chem.*, **74**, 2408 (1970).

voltage dependence as shown in Figure 3. Then eq 3 can be written

$$I_{ph} = k_4'(V)^{1.5}[R_w^+] \quad (3')$$

On substituting this into eq 7 we can relate photocurrent to incident light intensity, I_0

$$I_{ph} = \frac{k_4'k_2'}{k_3 + k_4'(V)^{1.5}} I_0 \epsilon C \sqrt{D\tau} V^{1.5} \times \exp\left\{-\frac{7m^2}{(k_4')^{3/2}kT}\left(\frac{I_{ph}}{V^{1.5}}\right)^{1.5} + \frac{f(V)}{kT}\right\} \quad (8)$$

An effective quenching term appears which is strongly dependent on light intensity. Figure 1 shows a plot of this equation (dotted line) for constant low applied voltage in a scale in which comparison to the experimental (solid) curve can be made. The fit was obtained by choosing parameters to make the curves match initially and at the 3% transmission point. Deviation between the dotted and solid curves is apparent only at high transmission. The experimental curve shows a somewhat greater rate of saturation, which is reasonable since no other quenching phenomena were considered in this derivation. Nor was any geometrical effect of an "excluded area" which is occupied by adsorbed rubrene cations included.

The existence of the intermediate state is consistent with the effect of an excluded area at high light intensities where the quenching can be large. The result is to have less than the full electrode area available for charge transfer. At increasingly higher fractional electrode coverage the photocurrent is expected to reach a true asymptotic limit as available space for charge transfer approaches zero. This is probably the main contributing effect which produces the shape of Figure 1 at the highest intensities. For a given range of incident light intensity higher applied voltage is expected to reduce saturation in this case also by reducing the lifetime of the intermediate state thereby making more electrode area available for charge transfer. This is qualitatively consistent also with the results of Table I and Figure 2. At lower fractional coverage the long-range dipole interaction energy is more important. As shown in Appendix II, when the dipole interaction energy is kT the spacing between cation centers is 44 Å. This corresponds to a surface coverage of only a few per cent for this molecule.

Equation 8 also predicts a decrease in the apparent quenching with an increase in applied voltage. In the limiting case of very high applied voltage the denominator approaches $k_4'V^{1.5}$, and the voltage dependence in numerator and denominator cancel. The exponential approaches unity and photocurrent becomes independent of applied voltage with value

$$I_{ph} \rightarrow k_2'\epsilon C\sqrt{D\tau} I_0 \quad (9)$$

This represents the unhindered conversion to photocurrent of the flux of rubrene singlets, where k_2' is the fraction of singlets quenched by the mechanism of charge transfer to the electrode. There is no saturation and for fixed wavelength the photocurrent depends only on incident light intensity. This is the condition which is being approached in Figure 2, where at 1000 V applied the divergence between curves has reached two orders of magnitude and presumably would eventually reach the expected three orders of magnitude at high enough applied voltage.

At the other limit of low applied voltage where the term $f(V)/kT$ is insignificant and the denominator of eq 8 is simply k_3, then the form of the equation is

$$\frac{I_{ph}}{V^{1.5}} = AI_0 \exp\left[-B\left\{\frac{I_{ph}}{V^{1.5}}\right\}^{1.5}\right] \quad (10)$$

The photocurrent is strongly quenched; and quenching is independent of applied voltage since the adsorbed ion-pair concentration at the wall, $[R_w^+]$, is determined only by recombination (rate constant k_3) and not by photocurrent production. The result is that photocurrent is proportional to $V^{1.5}$ for any intensity. Then for widely different intensities, log–log plots of photocurrent *vs.* applied voltage should be parallel with a slope of 1.5. This behavior is apparent also in Figure 2 for the range of low applied voltage.

For intermediate voltages and high intensity the lowering of the potential barrier to charge transfer expressed by $f(V)/kT$ becomes significant. This acts in a direction opposite to the photocurrent quenching term, $I_{ph}/V^{1.5}$, in the exponent of eq 8. This has the effect mathematically of making the photocurrent rise faster than $V^{1.5}$ in the range of voltage where $k_4'V^{1.5}$ is still small compared with k_3. The middle region of Figure 2 shows this behavior also. Our lack of explicit knowledge about details of the electrical double layer for this system precludes quantitative estimates of this effect.

The super-linear voltage dependence of photocurrent does not arise from the effects of space charge in the solution. This can be shown on the basis of magnitude of photocurrent for a given voltage. For example, for the experimental quantities: 100 V applied, 0.021-cm electrode spacing, mobility of 10^{-4} cm^2 V^{-1} sec^{-1}, and dielectric constant of 2.5, then substitution into the standard form for steady-state space charge limited current

$$H = 9\mu\epsilon/32\pi(V^2/L^3)$$

yields 3×10^{-8} A cm^{-2}. The measured values for graphs 3A and 3B converted to current density are approximately 3×10^{-12} A cm^{-2}, or four orders of magnitude lower. Therefore space charge limitations play no role in the nonlinearity of voltage dependence of photocurrent.

The ion-image intermediate state model for surface generated photocurrents appears, then, to be the only plausible model available to explain all of the experimental results obtained with benzene solutions of rubrene. It is felt, moreover, that these rubrene systems are not unique in their photoconducting properties. Therefore, this proposed mechanism should not be ignored when evaluating systems possessing photoconductive properties originating at electrode surfaces.

Appendix I

A reasonable model for dipole distribution on a conducting plate is sought. The two extreme cases are (a) dipoles are smeared out uniformly around the central dipole and (b) the dipoles are located on a lattice. Because of repulsion energy, m^2/r^3, case a is not valid since too much weight is given to near separations and because of Brownian motion case b cannot be completely valid. The elementary calculation which fol-

lows, based on cell theory of liquids in two dimensions, shows that for interaction energies of the order kT, case b actually is a good enough model, with minor corrections.

Let the effective number of nearest neighbors to a central dipole be smoothed out over a ring of dipoles. The dipoles are mutually parallel and all are perpendicular to the plane. In the spirit of cell theory these remain fixed and the central dipole is allowed to wander over the cell. Let r be the radial distance from the center to the central dipole and R be the radius of the ring. Dipole strength per unit ring circumference, ρ, is $Nm/2\pi R$, where N is the effective number of dipole nearest neighbors. Then the interaction energy between the central dipole and the ring of dipoles is

$$\epsilon = m\int_0^R \frac{\rho\, dl}{(R-r)^3} \tag{i}$$

where dl is the element of ring circumference. This can be written with the help of the cosine law as

$$\epsilon = \frac{Nm^2}{2\pi R^3} I\left(\frac{r}{R}\right) \tag{ii}$$

where

$$I\left(\frac{r}{R}\right) = \int_0^{2\pi} \frac{d\nu}{\left[1 + \left(\frac{r}{R}\right)^2 - 2\frac{r}{R}\cos\nu\right]^{3/2}}$$

and ν is the angle between vectors drawn from the origin to the central dipole and to a dipole element on the ring, respectively. Having energy, ϵ, as a function of the position in the cell of the central dipole, we can write the usual type of expression for average energy.

$$\bar{\epsilon} = \frac{\int \epsilon(r/R)\exp[-\epsilon(r/R)/kT]\, dA}{\int \exp[-\epsilon(r/R)/kT]\, dA} \tag{iii}$$

Equation ii is substituted and with minor manipulation gives eq iv where $x \equiv r/R$. The left side is the ratio of

$$\frac{\bar{\epsilon}}{Nm^2/R^3} = \frac{1}{2\pi}\frac{\int I(x)\exp\left[-\frac{Nm^2}{2\pi R^3 kT} I(x)\right] x^2\, dx}{\int \exp\left[-\frac{Nm^2}{2\pi R^3 kT} I(x)\right] x^2\, dx} \tag{iv}$$

average energy of the central dipole as it wanders over the cell divided by the energy of the central dipole fixed at r equals zero. The right side is clearly a function of R, the average (or lattice) spacing. The smaller the energy Nm^2/R^3, the larger will be the left-hand ratio, and the more smeared out the charge will be. But only for energies Nm^2/R^3 comparable to kT will there be significant reduction of photocurrent through production of a "back-field."

Equation iv is written for this special case, namely, when the rigid lattice interaction energy, Nm^2/R^3, equals kT.

$$\frac{\bar{\epsilon}}{kT} = \frac{1}{2\pi}\frac{\int_0^1 I(x)\exp\left[-\frac{1}{2\pi}\cdot I(x)\right] x^2\, dx}{\int_0^1 \exp\left[-\frac{1}{2\pi}\cdot I(x)\right] x^2\, dx} \tag{v}$$

The calculation was performed with the aid of a computer and the result is $\bar{\epsilon} = 1.86kT$. Therefore the average energy is not far removed from what is expected for a purely fixed lattice model.

Appendix II

The interaction of a central dipole pairwise with the rest of the lattice is

$$\epsilon = m^2 \sum_i 1/R_i^3 \tag{i'}$$

The sum is evaluated over the entire plane in a way similar to a Madelung constant calculation. If the dipoles are envisioned as placed in a square lattice, then around the central dipole there are: four nearest neighbors at a distance of R; four next neighbors at a distance $\sqrt{2}R$; four next neighbors at a distance $2R$; eight next neighbors at a distance $\sqrt{5}R$; four next neighbors at a distance $2\sqrt{2}R$; four next neighbors at a distance $3R$. For larger distances it is convenient to integrate. The number of dipoles in an annular ring of radius r and thickness dr is $2\pi r\, dr/R_1^2$. Then

$$\sum_{i>6}\frac{1}{R_i^3} \cong \int_{3R}^{\infty}\frac{1}{r^3}\frac{2\pi r\, dr}{R^2} = \frac{2\pi}{3R^3}$$

Therefore, collecting terms

$$\sum_i \frac{1}{R_i^3} = \frac{1}{R^3}\left(4 + \frac{4}{2^{3/2}} + \frac{4}{8} + \frac{8}{5^{3/2}} + \frac{4}{2^{9/2}} + \frac{4}{27} + \frac{2\pi}{3}\right) \tag{ii'}$$

which is approximately $7/R^3$. The interaction energy is $\epsilon \cong 7(m^2/R^3)$.

If we take dipole (ion-image) charge separation to be 5 Å, then an interaction energy of kT at room temperature results when R is 48 Å. Two factors have been omitted, the dielectric constant of 2.5 and the factor of 1.86 calculated in Appendix I. If these are inserted, the distance R is shortened only slightly to 44 Å. Since their effect is not large, both quantities were omitted in the calculation of the text.